

Cost-Effective early warning solution for Anisocoria Eye-Disease through Optical Sensing and Machine Learning: A Preliminary Analysis

1st Mohd Mansoor Khan

*Department of Electronics and Communication Engineering
Indian Institute of Information Technology Guwahati
Guwahati-781015, Assam, India
mansoor@iiitg.ac.in*

2nd Priyam Raj

*Department of Electronics and Communication Engineering
Indian Institute of Information Technology Guwahati
Guwahati-781015, Assam, India
priyam.raj@iiitg.ac.in*

3rd Sanu Kumar

*Department of Electronics and Communication Engineering
Indian Institute of Information Technology Guwahati
Guwahati-781015, Assam, India
sanu.kumar@iiitg.ac.in*

Abstract—Anisocoria is the medical term associated when one of the pupil's radius is not equal to the other one. This often leads to disease occurrence in the human eye when it remains undetected in its “silent” early phases. Therefore, this paper proposes a prototype of a low-cost early-warning anisocoria detection system by sensing and measuring the pupil diameter in the human eye. The unprocessed human-eye images were transformed to efficiently detect the pupil's circumference using image binarization, leveling, and Hough transform techniques. Applying the machine learning (ML) algorithms using logistic regression, the model was trained and tested on the data set consisting of 75 random eye images. The prediction accuracy achieved was 81% when tested under red, green, blue, and ambient illumination. Furthermore, the proposed method was compared with the two other image processing methods, namely the Canny edge and Daugman algorithms, for optimum selection at the pre-ML stage. This method could prove to be a cost-effective solution for early diagnosis of anisocoria vis-a-vis database production to further accurate the proposed sensor system.

Index Terms—Anisocoria, Pupil Detection, Image Processing, Machine Learning

I. INTRODUCTION

The light propagates through the eye by entering the cornea and passing to the pupil, which acts as a natural aperture to the iris. The optical information is sent to the brain via the optic nerve while passing through the iris and converged at a focal point by a lens. The basic anatomy of the human eye is shown in Fig. 1 [1], [2]. The pupil is a muscular annular disc attached to the eye's iris. The aperture diameter is controlled to accommodate the optical flux entering the retina. Apparently, over time, the pupil aperture dimensions and its response to optical illumination may vary from their normal values owing to certain diseases. This condition affects the typical accommodation of the eye, which may be due to abnormal brain-eye signaling and cognitive processing [3]. Therefore, a comprehensive study on eye-related diseases has been carried

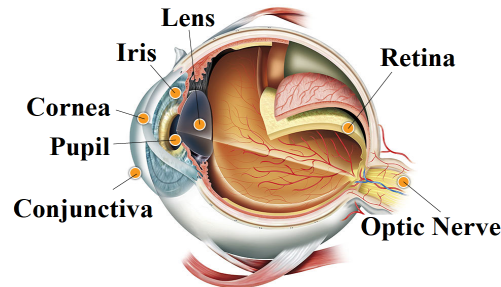


Fig. 1. Basic anatomy of a human eye highlighting the position of pupil

out to identify the pupillary conditions as presented in Table I.

TABLE I
SURVEY ON TYPICAL EYE RELATED DISEASES.

Eye Condition	Attributes and Symptoms	Remarks
Anisocoria	<ul style="list-style-type: none"> Parkinson's and Horner's syndrome Larger pupillary diameter Longer latency and contraction time Reduced contraction amplitude Impaired reaction to stimulation 	[4]–[6]
Holmes-Adie Syndrome	<ul style="list-style-type: none"> Inflamed ciliary ganglion Pupil always dilated Ovaly distorted pupil Blurry vision and photophobia 	[7]
Ross Syndrome	<ul style="list-style-type: none"> Adie pupil Loss of tendon reflexes Heat intolerance 	[7]
Rieger's Anomaly	<ul style="list-style-type: none"> Clouding of cornea edges Distorted pupil Displaced iris tissues 	[7]
Anterior Uveitis	<ul style="list-style-type: none"> Inflammation of iris Pathological pupil distortion Pharmacological pupil dilation Iris atrophy due to synechiae 	[8]

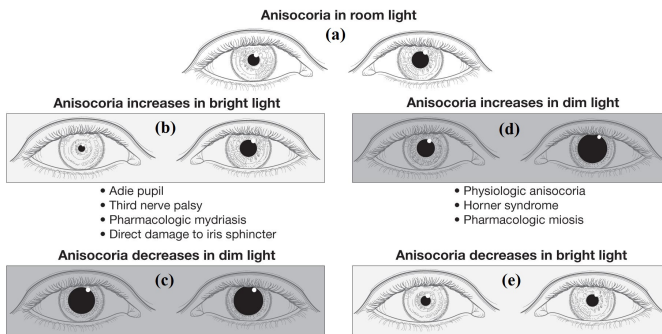


Fig. 2. Illustrative representation of anisocoria under (a) ambient room illumination, (b) it increases in bright illumination scenario, which in some cases decreases when the light intensity is diminished (c), (d)–(e) shows the reverse effects observed in (b)–(c).

It can be observed that various diseases can be diagnosed with symptoms that can appear in one or both the eye pupils indicating abnormalities including alcohol and drug addiction [9]. Anisocoria is a major global health problem and is only the second leading cause of blindness worldwide. It is estimated to be over 20% of the population with the disease at initial undetected (silent) phase [10], [11]. It can be observed in the illustration of Fig. 2 that anisocoria is dynamic with respect to illumination conditions (ambient, bright, dim, and wavelength dependent) and may vary as per the individual patient [4]–[6]. Consequently, cost-effective early detection of pupil disorders leading to anisocoria disease would be a boon to the financially weak sections of human society.

As per the literature studies, to design and prototype the pupillary measurement and classification system for anisocoria, the optoelectronics sensor and system approach is considered optimal [3], [12]–[15]. In fact, with optoelectronics sensing, various other human body measurement parameter systems have been developed and prototyped in the past [16]–[18]. Consequently, various laboratory measurement prototypes and commercial pupillometers have been developed for dynamic and static recording of pupil's diameters and their response to illumination [3], [12]–[15]. Of them, monocular and binocular pupillometry were considered to form the basics of eye image acquisition, processing, and sensing [9], [12], [19]. Binocular measurement is considered to be better suited for research and clinical applications than the monocular [12]. However, if the optical source is uniformly distributed, a monocular pupillary measurement system may prove to be

cost-effective for a preliminary warning system to anisocoria. The binocular system employs a high-resolution camera for capturing the image apart from peripheral optics making them comparatively costly and non-movable lab-ridden devices [9], [12], [14].

To overcome the aforementioned challenges of high-cost factors and portability, a real-time prototype sensing system for anisocoria detection has been proposed in this paper. It would also be beneficial in producing a database for training and testing the model to better the testing accuracy. The flowchart shown in Fig. 3 describes the optical source, which is a laptop screen with 100% brightness to mimic the uniform and distributed optical source consisting of white, red, blue, and green sources. The human subject's pupilary response shall be received by the optical detector. It will further send the image for processing to the processor and ML algorithm to detect anisocoria.

II. THEORY AND METHODOLOGY

It can be observed in Fig. 3 that the pupil sensing and measurement system proposed in this work, primarily consist of image acquisition, processing, ML training, and testing. This section describes primarily the image processing algorithms employed in the presented work with its corresponding ML training/testing.

A. Image Acquisition and Processing

As shown in Fig. 3, the optical source with various wavelengths in the visible range act as a stimulus to the human eye to produce a response that is been captured by the camera. The acquired image is then sent to the processor for pupil circumference identification and measurement. Various image processing algorithms have been tested on the camera images to select the optimum process with the highest accuracy of measurement. All the algorithms were tested on a 75 image database.

1) Algorithm-1: Canny Edge and Hough Transform: The Viola-Jones approach has been applied to isolate the eye region from the face from an input gray-scale converted image [20]. The gray scale reduces the computational complexity of processing the image and removes redundant features such as unusual facial expressions, occlusions, and media quality parameters owing to non-uniform illumination. Owing to the lack of an explicit database for anisocoria diseased eye, an input image used in this work is a profile image with a healthy eye that has been fetched from Siblings Image Database (SiblingsDB) with a pixel resolution of 350×350 [21]. It contains images of individuals with sibling relationships. The images are categorized into profile pictures with and without expressions (56) captured professionally with uniform and controlled illumination conditions. The images belong to the voluntary students, employees, and their respective siblings of Politecnico di Torino with an average age of 23.1 years ranging between 13–50 years. The 57% of the total images belong to male Caucasians and were not wearing any make-up or cosmetics. The Canny edge detection algorithm

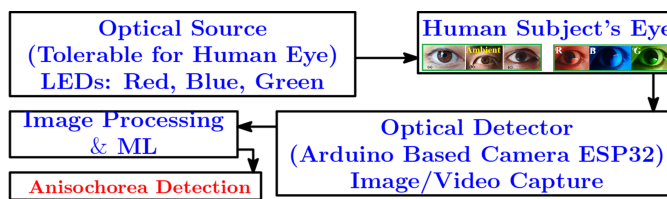


Fig. 3. Flow working of the proposed pupil sensing system for anisocoria detection.

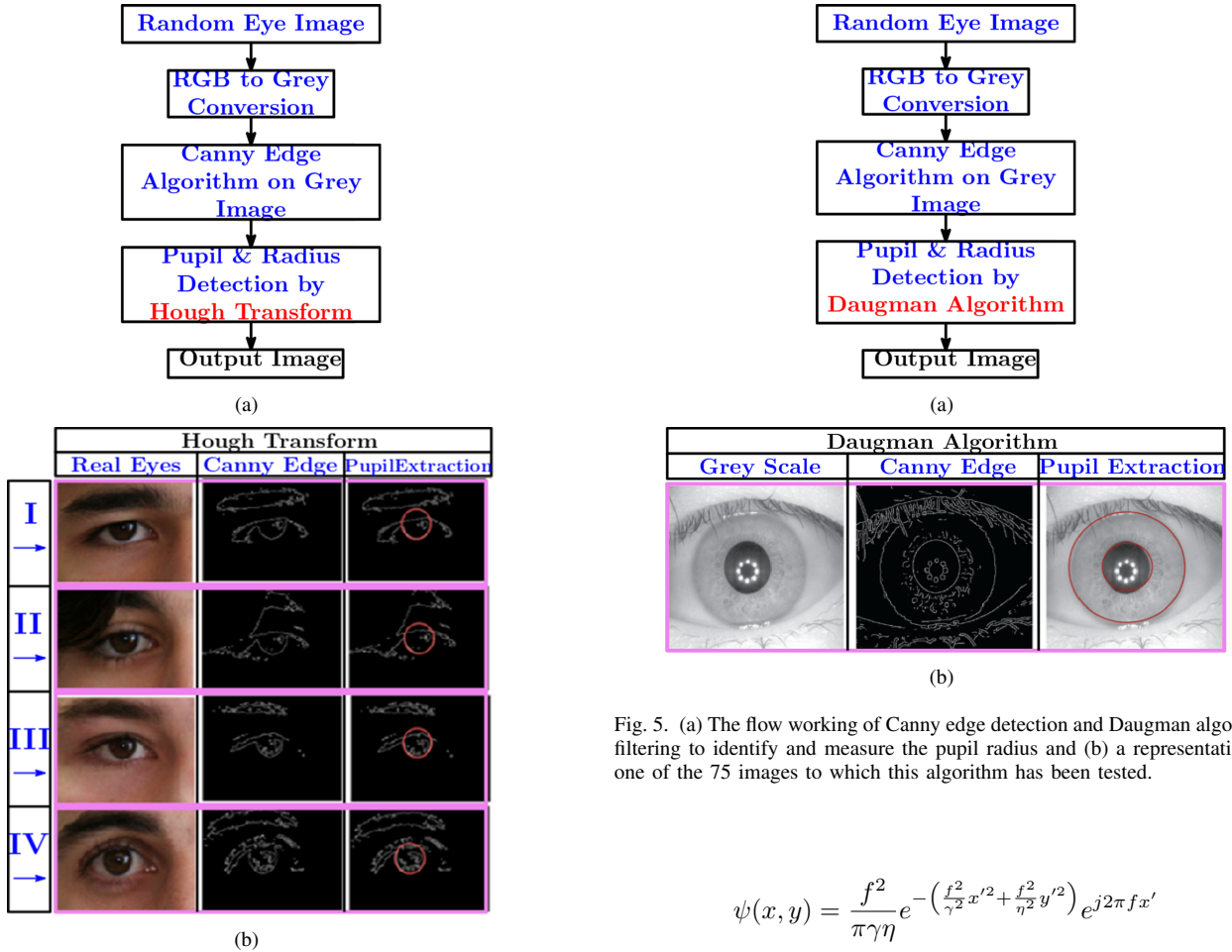


Fig. 4. (a) The flow working of Canny edge detection and Hough transform to identify and measure the pupil radius and (b) a set of four-eye image implementation (I-IV).

uses a linear filtering approach that smooths the noise and computes the edge strength for each pixel [22]. Furthermore, to localize the iris, the integro-differential operators with Hough transform have been employed that are based on the concept of instantaneous phase or emergent frequency for feature extraction presented in the output image [23]. This process can be summarized in the flowchart shown in Fig. 4 (a) with the corresponding four-image set example onto which the process has been applied as shown in Fig. 4 (b). This method is computationally exhaustive, leading to low-speed efficiency.

2) *Algorithm-2: Canny Edge and Daugman Algorithm:* This approach also employs integro-differential operators to determine the iris center and diameter after edge detection. The pupil is detected using differential operators [23]. The feature extraction uses two-dimensional (2D) Gabor wavelet filtering, which proved efficient in the cells of the mammalian visual systems. It is composed of a bank of linear band-pass filters to which impulse response is obtained by a product of harmonic (complex sinusoidal plane of a particular frequency) and Gaussian functions given as [24], [25]

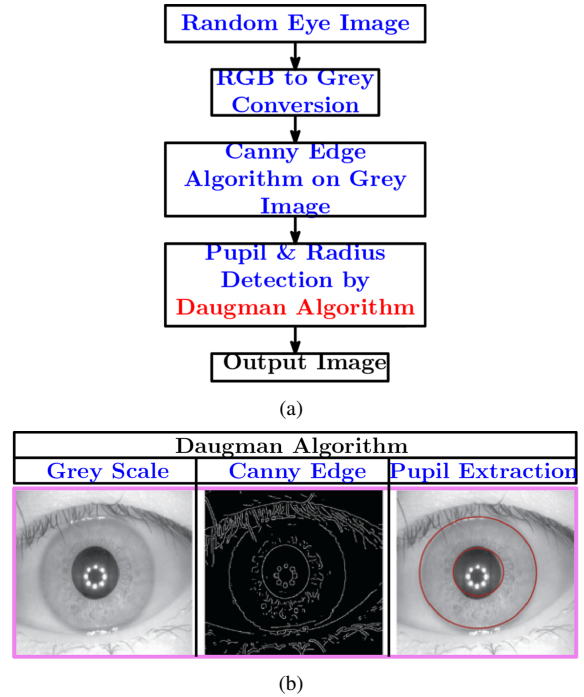


Fig. 5. (a) The flow working of Canny edge detection and Daugman algorithm filtering to identify and measure the pupil radius and (b) a representation of one of the 75 images to which this algorithm has been tested.

$$\psi(x, y) = \frac{f^2}{\pi\gamma\eta} e^{-\left(\frac{f^2}{\gamma^2}x'^2 + \frac{f^2}{\eta^2}y'^2\right)} e^{j2\pi fx'} \quad (1)$$

$$x' = x \cos \theta + y \sin \theta \quad (2)$$

$$y' = -x \sin \theta + y \cos \theta \quad (3)$$

where, f , η , γ , and θ are the filter's central frequency, sharpness perpendicular to the plane wave (minor axis), sharpness along the major axis, and Gaussian major axis rotation angle to the plane wave respectively. It can be observed in the flowchart of Fig. 5 (a) that the grey converted image is Canny edge detected. The pupil extraction and radius detection have been carried out using Daugman's Algorithm filters to produce the output image as shown in Fig. 5 (b).

3) *Algorithm-3: Binerization, Labeling, and Hough Transform:* A review of the relevant literature suggests that the method with high contrast between the dark intensity of the pupil region and the bright sclera region is commonly used for pupil detection. Therefore, image thresholding and binarization techniques have been employed to localize the pupil. The binary image is obtained from gray image intensity $[I(x, y)]$ by obtaining a grey level histogram (0–255 levels) and their corresponding pixel populations as shown in Fig. 6 (a). Apparently, the pupil is isolated from other features using the identified threshold value (T). This value is further used to convert the grey image into its binary form $[B(x, y)]$ using the expression [26]

$$B(x, y) = \begin{cases} 1, & \text{if } I(x, y) < T \\ 0, & I(x, y) \geq T \end{cases} \quad (4)$$

Furthermore, post-binariization, a labeling technique, eliminates the pixels with noise. The different color scheme is used after subtraction of adjacent similar intensity areas containing the pixels as shown in Fig. 6 (b) [26]. The Hough circle algorithm calculates the pupil aperture radius in the ambient day, red, blue, green, and under no-light conditions. Consequently, it can be observed in Fig. 7 (a) and (b) the flow working and an eye image to which this combinational algorithm has been applied. The standard eye data set, which has been obtained by using algorithms 1–3, is then fed to the training/testing of the ML algorithm to find the detect efficiency of anisocoria.

B. Machine Learning

Automatic learning from the patterns in the data without structuring them is achieved using machine learning (ML) approaches in artificial intelligence (AI). Apparently, various ML algorithms are based on data-demanding neural networks, support vector machines, recurrent neural networks, and random forest classifiers [27]–[30]. However, using logistic regression (LS), the probability of the output variable is mapped to its appropriate category and determines the resolution of the images. Various literature suggests LS as the best possible predictor, and classification model [28]. Therefore, in this work, the designed ML model employs the LR technique to train the model with five categories of pupil aperture radii enumerated below

- 1) Ambient white light radius (x_1)
- 2) Ambient red light radius (x_2)
- 3) Ambient blue light radius (x_3)
- 4) Ambient green light radius (x_4)
- 5) Dark radius (x_5)

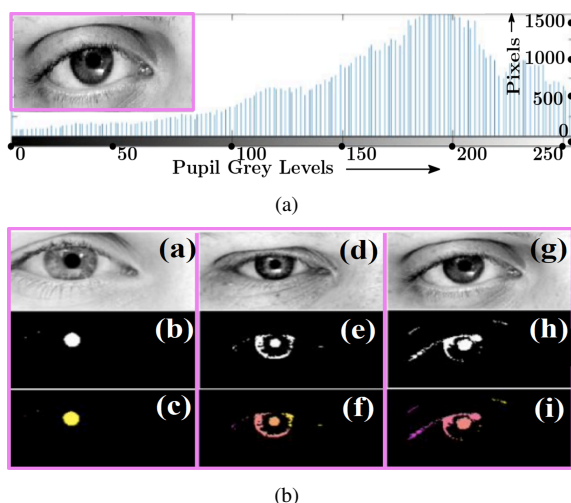
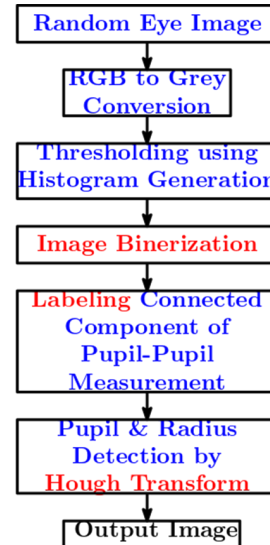
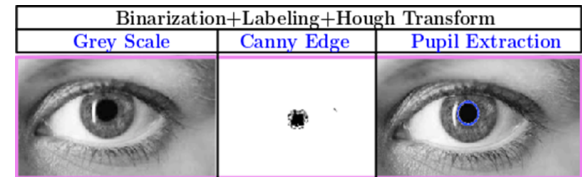


Fig. 6. (a) The process of image binerization using histogram creation from its grey scale values and (b) a representation of 3-set labeled images obtained after the process of binerization.



(a)



(b)

Fig. 7. (a) The flow working of binarization, labeling, and Hough transform combinational algorithm to identify and measure the pupil radius and (b) a representation of one of the 75 images to which this algorithm has been tested.

The tuple data set $(x_1, x_2, x_3, x_4, x_5)$ was used to train algorithms 1–3, and the corresponding testing accuracy was determined to evaluate the optimum performance for the hardware implementation of the sensing system.

III. EXPERIMENTAL SETUP

The prototype of the pupillary sensing system consists of image acquisition and its processing using ESP 32 camera and Arduino processor, respectively. The processor is utilized for pupil aperture radius calculation, training the ML model on the acquired data set, and testing the human subject's eye image to detect anisocoria disease. The experimental setup is shown in Fig. 8. The components required to fabricate the prototype model are mentioned in Table II.

TABLE II
COMPONENT SPECIFICATIONS FOR PROTOTYPE DEVELOPMENT

Component	Make	Specifications
Distributed Optical Source (Laptop Screen)	hp	14 inch screen (Full Brightness)
Processor	Atmel	ATmega2560 ESP8266
Camera	ESP32-CAM Development Board	OV2640 Camera Module
Image Database	SiblingDB	350×350 pixels

The ESP32 camera with WiFi module was synced with the Arduino processor to acquire and transfer the images. Depending upon the accuracy results (described in the next section) of the ML algorithms, the relevant process was burnt to the processor to process the image and issue a warning for the anisocoria disease.

IV. RESULTS AND DISCUSSIONS

The outputs of the 75 image data set obtained from algorithms 1–3 were used to train and test the ML model based on the logistic regression approach. The radii values of the pupil aperture obtained from the output images after the Hough transform from algorithm-3 detected the accuracy of 81% true detection in the ML analysis. It can be observed from Fig. 9 the value of the dark radius calculated as 3.745 mm from the algorithm-3 which typically is 2–4 mm in diameter in bright light to 4–8 mm in the dark [31]. The radii values from the image outputs of algorithms 1 and 2 correspondingly provided the true detection accuracies of 40% and 60% respectively.

The LR approach for the ML training/testing using the outputs from algorithm-3 gave the true accuracy of 81% when trained for 5-tuple data (x_1, x_2, x_3, x_4, x_5) as shown in Fig. 10. Apparently, this accuracy is not enough for clinical diagnostics compared to the existing state-of-the-art technologies with better accuracies of more than 95% but with higher costs and bulky setups [9]–[12], [14]. However, considering the cost-effective early warning anisocoria sensing system, the detection accuracy can be further optimized with actual disease data set training and testing. The total cost of the developed prototype was calculated approximately as US\$ 20.00 (1600.00 Indian National Rupee), which is comparatively far less than the commercially available pupillary sensing systems.

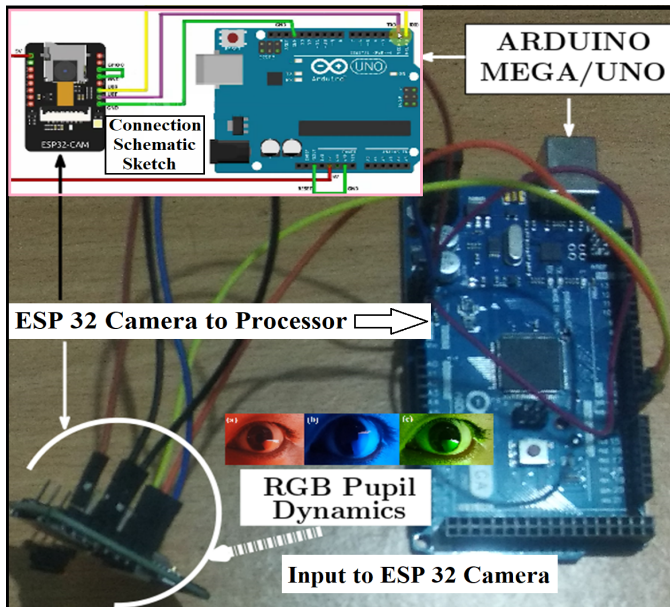


Fig. 8. Experimental setup of to detect anosocoria using the developed prototype model.

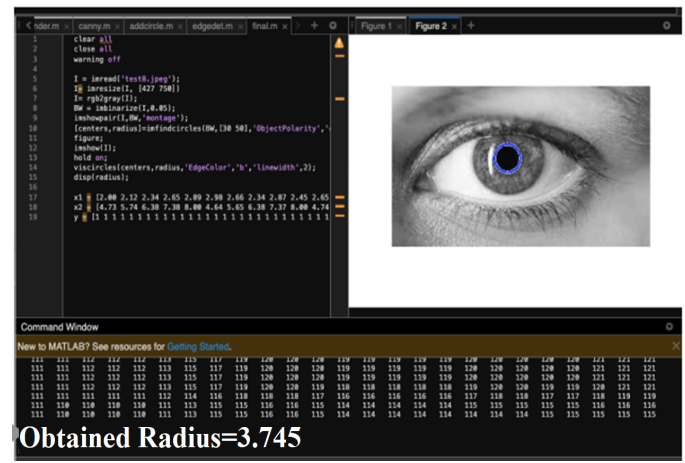


Fig. 9. Pupil radius identification and distribution after application of Hough transform in algorithm-3.

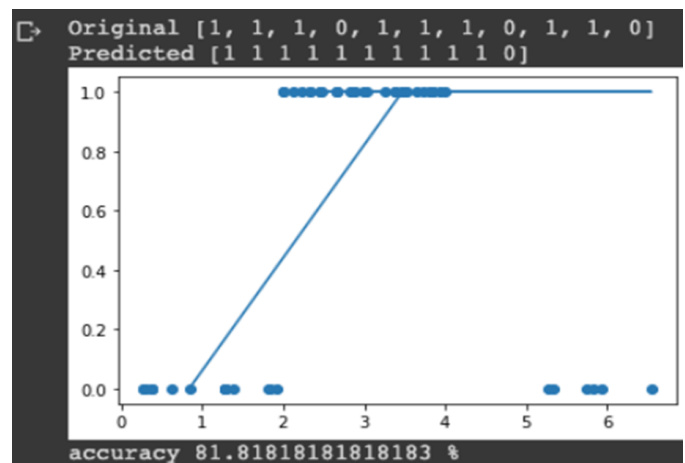


Fig. 10. The logistic distribution training on the radii values of the pupil obtained from algorith-3.

Consequently, the improved version of this system can be utilized in detecting anisocoria disease in the rural areas of developing countries.

V. CONCLUSIONS

This paper proposes a cost-effective early warning system for anisocoria eye disease through optical sensing and machine learning. The pupil aperture radius detection and measurement have been performed through a developed prototype model. The radii values were obtained from three algorithms 1–3, presented in this work. The true detection accuracy has been obtained as 81% through the logistic regression machine learning process, which was trained/tested on 75 images data set. One of the factors that also affect the result is that not all images have the same quality. The prototype is low-cost and portable, which could prove to be a pivotal factor for the economically underprivileged population in developing countries suffering from anisocoria that cannot reach costly medical diagnostics.

In the future, a database that will contain images of people with and without anisocoria should be created. Images will be taken under controlled conditions that will, for sure, affect testing result accuracy and improve the algorithm–3 performance.

REFERENCES

- [1] M. O. Hughes, "A pictorial anatomy of the human eye/anophthalmic socket: a review for ocularists," *eye*, vol. 4, no. 5, pp. 51–63, 2007.
- [2] ——, "Anatomy of the anterior eye for ocularists," *J Ophthalmic Prosthet*, vol. 8, pp. 25–35, 2004.
- [3] L. Peretto, L. Rovati, G. Salvatori, R. Tinarelli, and A. E. Emanuel, "A measurement system for the analysis of the response of the human eye to the light flicker," *IEEE transactions on instrumentation and measurement*, vol. 56, no. 4, pp. 1384–1390, 2007.
- [4] G. Micieli, C. Tassorelli, E. Martignoni, C. Pacchetti, P. Bruggi, M. Magri, and G. Nappi, "Disordered pupil reactivity in parkinson's disease," *Clinical Autonomic Research*, vol. 1, pp. 55–58, 1991.
- [5] C. C. Chan, M. Paine, and J. O'Day, "Carotid dissection: a common cause of horner's syndrome," *Clinical & Experimental Ophthalmology*, vol. 29, no. 6, pp. 411–415, 2001.
- [6] J. Upshaw, B. MacLean, and J. D. Losek, "Anisocoria and topical carbamate exposure: illustrative case report," *Clinical pediatrics*, vol. 49, no. 5, pp. 502–505, 2010.
- [7] M. S. Sarao, A. G. Elnahry, and S. Sharma, "Adie syndrome," in *StatPearls [Internet]*. StatPearls Publishing, 2022.
- [8] T. M. Aslam, S. Z. Tan, and B. Dhillon, "Iris recognition in the presence of ocular disease," *Journal of The Royal Society Interface*, vol. 6, no. 34, pp. 489–493, 2009.
- [9] D. Iacoviello, "Analysis of pupil fluctuations after a light stimulus by image processing and neural network," *Computers & Mathematics with applications*, vol. 53, no. 8, pp. 1260–1270, 2007.
- [10] A. Basit, M. Javed, and S. Masood, "Non-circular pupil localization in iris images," in *2008 4th International Conference on Emerging Technologies*. IEEE, 2008, pp. 228–231.
- [11] W. N. Payne, K. Blair, and M. J. Barrett, "Anisocoria," in *StatPearls [Internet]*. StatPearls Publishing, 2022.
- [12] W. Nowak, A. Żarowska, E. Szul-Pietrzak, and M. Misiuk-Hojoł, "System and measurement method for binocular pupillometry to study pupil size variability," *Biomedical engineering online*, vol. 13, no. 1, pp. 1–16, 2014.
- [13] W. P. Van Der Meijden, B. H. Te Lindert, J. R. Ramautar, Y. Wei, J. E. Coppens, M. Kamermans, C. Cajochen, P. Bourgin, and E. J. Van Someren, "Sustained effects of prior red light on pupil diameter and vigilance during subsequent darkness," *Proceedings of the Royal Society B: Biological Sciences*, vol. 285, no. 1883, p. 20180989, 2018.
- [14] L.-L. Lobato-Rincón, M. d. C. Cabanillas-Campos, C. Bonnin-Arias, E. Chamorro-Gutiérrez, A. Murciano-Cespedosa, and C. Sanchez-Ramos Roda, "Pupillary behavior in relation to wavelength and age," *Frontiers in human neuroscience*, vol. 8, p. 221, 2014.
- [15] W. Nowak, A. Żarowska, E. Szul-Pietrzak, and A. Hachol, "Measurement system for pupil size variability study," in *XIII Mediterranean Conference on Medical and Biological Engineering and Computing 2013: MEDICON 2013, 25-28 September 2013, Seville, Spain*. Springer, 2014, pp. 1583–1586.
- [16] M. Zhang, Z. Zhang, D. Yuan, S. Feng, and B. Liu, "An automatic gas-phase molecular absorption spectrometric system using a uv-led photodiode based detector for determination of nitrite and total nitrate," *Talanta*, vol. 84, no. 2, pp. 443–450, 2011.
- [17] S. Debarshi and M. M. Khan, "Portable and low-cost led based spectrophotometer for the detection of nitrite in simulated-urine," in *2019 International Conference on Electrical, Electronics and Computer Engineering (UPCON)*. IEEE, 2019, pp. 1–4.
- [18] Y. Yamakoshi, M. Ogawa, T. Yamakoshi, M. Satoh, M. Nogawa, S. Tanaka, T. Tamura, P. Rolfe, and K.-i. Yamakoshi, "A new non-invasive method for measuring blood glucose using instantaneous differential near infrared spectrophotometry," in *2007 29th Annual International Conference of the IEEE Engineering in Medicine and Biology Society*. IEEE, 2007, pp. 2964–2967.
- [19] A. Hachol, W. Szczepanowska-Nowak, H. Kasprzak, I. Zawojńska, A. Dudzinski, R. Kinasz, and D. Wygledowska-Promienna, "Measurement of pupil reactivity using fast pupillometry," *Physiological measurement*, vol. 28, no. 1, p. 61, 2006.
- [20] T. Paul, U. A. Shamm, M. U. Ahmed, R. Rahaman, S. Kobashi, and M. A. R. Ahad, "A study on face detection using viola-jones algorithm in various backgrounds, angles and distances," *International Journal of Biomedical Soft Computing and Human Sciences: the official journal of the Biomedical Fuzzy Systems Association*, vol. 23, no. 1, pp. 27–36, 2018.
- [21] T. F. Vieira, A. Bottino, A. Laurentini, and M. De Simone, "Detecting siblings in image pairs," *The Visual Computer*, vol. 30, pp. 1333–1345, 2014.
- [22] L. Ding and A. Goshtasby, "On the canny edge detector," *Pattern recognition*, vol. 34, no. 3, pp. 721–725, 2001.
- [23] J. G. Daugman, "High confidence visual recognition of persons by a test of statistical independence," *IEEE transactions on pattern analysis and machine intelligence*, vol. 15, no. 11, pp. 1148–1161, 1993.
- [24] J.-K. Kamarainen, V. Kyrki, and H. Kalviainen, "Invariance properties of gabor filter-based features-overview and applications," *IEEE Transactions on image processing*, vol. 15, no. 5, pp. 1088–1099, 2006.
- [25] T. Barbu, "Gabor filter-based face recognition technique," *Proceedings of the Romanian Academy*, vol. 11, no. 3, pp. 277–283, 2010.
- [26] N. Corovic and E. Arslan, "An implementation that diagnosis anisocoria disease using image processing techniques," *Uludağ Üniversitesi Mühendislik Fakültesi Dergisi*, vol. 25, no. 1, pp. 555–572, 2020.
- [27] T. Rymarczyk, E. Kozłowski, G. Kłosowski, and K. Niderla, "Logistic regression for machine learning in process tomography," *Sensors*, vol. 19, no. 15, p. 3400, 2019.
- [28] S. Nusinovici, Y. C. Tham, M. Y. C. Yan, D. S. W. Ting, J. Li, C. Sabanayagam, T. Y. Wong, and C.-Y. Cheng, "Logistic regression was as good as machine learning for predicting major chronic diseases," *Journal of clinical epidemiology*, vol. 122, pp. 56–69, 2020.
- [29] F. Thabtah, N. Abdelhamid, and D. Peebles, "A machine learning autism classification based on logistic regression analysis," *Health information science and systems*, vol. 7, pp. 1–11, 2019.
- [30] M. M. Khan, P. Jaiswal, M. Mishra, and R. K. Sonkar, "Strategic-cum-domestic vehicular movement detection through deep learning approach using designed fiber-optic distributed vibration sensor," in *2022 IEEE 7th International conference for Convergence in Technology (I2CT)*. IEEE, 2022, pp. 1–6.
- [31] H. K. Walker, W. D. Hall, and J. W. Hurst, "Clinical methods: the history, physical, and laboratory examinations," 1990.